



Research Article

A Hybrid Technique for Fault Classification and Location in a Jointed Overhead-Underground Distribution Line

Dorothy W. Gicheru, Edwell T. Mharakurwa, Waweru Njeri

Department of Electrical and Electronic Engineering, Dedan Kimathi University of Technology, Private Bag 10143, Nyeri, Kenya

ARTICLE INFORMATION

Received: July 24, 2023
 Revised: August 16, 2023
 Accepted: September 18, 2023
 Available online: November 26, 2023

KEYWORDS

ANFIS, Jointed Overhead-Underground Line, Discrete Wavelet Transforms, Multilayer Perceptron, Artificial Neural Network

CORRESPONDENCE

Phone: +254 759898246
 E-mail: dorothy.gicheru@dkut.ac.ke

A B S T R A C T

The electrical distribution system is crucial for the utility grid to transmit power from generators to consumers. Considering the intricate structure of distribution systems and their significant role in power networks, establishing a robust fault classification and location scheme is vital. Due to ageing, distribution systems are often prone to faults from factors like poor operational conditions and wear and tear. The line faulting rate and the pertinent restoration epochs influence the frequency and duration of power disruptions. Thus, precisely locating the fault section is essential to minimize power restoration timeframes. This paper presents a hybrid fault classification and location technique in a combined continuous overhead and underground distribution line. A simulation of the hybrid model was designed in Simulink for an 11 kV combined continuous overhead and underground electrical distribution line, considering short circuit faults as they are the most predominant and cause massive damage in distributed systems. The proposed technique first classifies the fault using Discrete Wavelet Transforms (DWT) and Multi-layer Perceptron-Artificial Neural Networks (MLP-ANN). Next, the impedance and Adaptive Neuro-Fuzzy System (ANFIS) based technique is employed for fault location. At a sample rate of 50 kHz, the DWT was applied to current signals and the coefficients used for ANN training, while phase impedance values were used as input to the ANFIS for training. The simulation results showed accuracy of 96.6% for fault classification and 99.17% for fault location. The developed models can significantly enhance fault location for speedier outage resolution by promptly repairing the affected distribution lines.

INTRODUCTION

Transmission and distribution lines are integral links of any electrical grid system that enable the permanence and continuity of energy from the generating source to the end users [1]. Just like any other electrical equipment, distribution lines are susceptible to faults. Faults disrupt the smooth flow of electricity, and they include, but are not limited to, short circuits, ground faults, open circuits, overloads, and transient faults. Short circuits are often the most predominant and require significant attention in fault management strategies. Short circuits typically occur due to a direct connection between two conductors with differing potentials, resulting in an excessive current flow. These faults pose immediate and severe risks to the electrical system, potentially leading to equipment damage, power outages, and safety hazards. As a result, short circuit faults demand proactive control measures to safeguard the integrity and stability of the power distribution network [2].

Traditionally, overhead cables have been utilized to transmit and distribute electrical power. As a result of continued exposure to the outside atmosphere, overhead lines have various issues with safety and dependability. Nonetheless, overhead lines' most distinct benefits include lower costs due to lower insulation levels

required, simplicity of fault diagnosis due to a clear view of the conductors, lower installation costs, and ease of extension [3].

Recently, there has been a rapid surge in the demand for electrical energy in urban areas. Worldwide, there is a growing trend of replacing overhead distribution lines with extensive underground power cables, particularly in environmentally sensitive and densely populated regions. Moreover, underground cables reduce the risk of failure caused by external factors such as rain, wind, and harsh weather conditions. Radio interference is also not present in underground wires [4]. However, underground cables are also susceptible to faults due to exposure to overload, ageing, mechanical, electrical, or chemical stress [5]. Also, faults in underground cables are difficult to detect, and restoring the system once faults are discovered may take a long time for the same electric power capacity as an overhead cable system.

Recently, attention has been directed towards jointed overhead and underground electrical power distribution cable technology. This shift in focus is driven by evolving perceptions of the electrical power system engineers, considering reliability, safety, and economic factors [2]. Combined overhead and underground cables are also susceptible to faults; thus, asset managers need to adopt techniques that can accurately detect and locate faults when

they to happen. Prompt fault classification, location, and restoration are crucial tasks of the power systems asset managers to avert losses that can be accrued due to energy discontinuity.

The need for fault classification and location research studies has increased significantly in recent years due to the growing complexity of contemporary power transmission and distribution systems [6]. Identifying the existence and pinpointing the exact location of a fault is a critical element in effective fault management as it speeds up the process of restoring energy and guaranteeing the system's stability. The precise location of the fault will allow prompt repair, lower operating costs, improve system accessibility, and reduce crew time and expense required to traverse hazardous terrain [7]. Researchers have categorized the established transmission or distribution line fault classification and location methodologies into two clusters: traditional and soft computing-based techniques [3–5].

Conventional Approaches for fault detection and location

Conventional fault classification and location approaches encompass a set of well-established techniques. These methods primarily include impedance-based strategies and travelling wave techniques. Impedance-based techniques are straightforward and rely on monitoring the line's current, voltage, and resistance values before or after a fault occurs [1], [7] – [10]. In contrast, travelling wave techniques analyze voltage and current signals both pre- and post-fault to extract valuable fault signatures for classification and location purposes [11] – [13]. One of the notable advantages of impedance-based techniques is their simplicity and the use of readily available parameters, making them practical for various distribution systems. On the other hand, travelling wave techniques excel in multi-branched radial distribution topologies, offering valuable insights into fault location. However, these approaches are not without their challenges [7].

Determining fault locations in combined overhead-underground networks using impedance-based methods can be complex, primarily due to non-homogeneous impedance characteristics between underground cables and overhead lines. Additionally, travelling wave techniques must contend with varying propagation velocities of combined lines' travelling waves, which can complicate the identification of fault zones [9]. Conventional approaches find their applications in fault detection across a broad spectrum of power distribution systems, particularly in scenarios where simplicity and reliability are paramount [9].

Soft-Computing-Based Approaches for fault detection and location

In contrast to conventional methods, soft-computing-based fault detection approaches leverage advanced technologies and intelligent algorithms. This cluster includes techniques such as Artificial Neural Networks (ANN) [14], Support Vector Machines (SVM) [15], fuzzy logic [16], [17], and Genetic Algorithms (GA) [18], [19]. These techniques rely on machine learning and data analysis to interpret fault data effectively.

The advantages of soft computing techniques lie in their adaptability to changing conditions and robust fault detection capabilities. They excel in handling complex data and possess the

capacity for self-learning and adaptation. However, these techniques do have their own set of challenges. They heavily depend on training data, and any changes in the network configuration may necessitate new data acquisition and algorithm updates. Furthermore, the performance of these methods can be influenced by the quality and quantity of available training data [20]. Soft-computing-based techniques are particularly well-suited for scenarios where adaptability to evolving fault patterns and a higher degree of automation are required, making them valuable tools in modern, complex distribution systems.

Research has been geared towards improving stand-alone and hybrid fault classification and localization techniques. Fuzzy logic has been exploited in fault locations for combined transmission lines [21], [22]. However, there are difficulties in optimizing the fuzzy logic network parameters. An adaptive neural network-fuzzy technique is utilized in [23] to detect, classify, and correctly locate faults in a combined transmission system using essential components of post-fault-recorded voltages.

In reference [24], the authors used wavelet and fuzzy algorithms to locate abnormalities in a single-core underground power cable. The wavelet transform extracts features from the fault signal, and fuzzy logic was utilized to pinpoint the fault. This model offered an acceptable level of accuracy but there is need to examine the vast range of fault scenarios to test its robustness. In the hybrid method described in reference [25], SVM is used to identify the fault region after the DWT has extracted the transient characteristics from recorded voltages. However, in this method, the losses at the joints between overhead and underground cables are assumed to be negligible. A fault location methodology based on neuro-fuzzy systems in jointed transmission lines with underground power cables is proposed in [26]. Although the authors managed to get accurate results, the method only addressed a single line-to-ground fault. Thus, to improve the efficacy of this method other types of faults must not be overlooked.

A detailed comparison of fault location algorithms is conducted in reference [3], focusing on long transmission lines combined with underground cables. The authors aimed to achieve precise fault location by implementing a hybrid system that combines impedance-based and wavelet-based techniques. It is worth noting that, while achieving impressive accuracy, the study relies on data from both sending and receiving ends, which may not always be available in practical applications. However, combining Modal Transformation, Wavelet Transform, and ANN showcased the potential for significantly improved fault location accuracy by integrating multiple techniques. In particular, the combination of Wavelet Transform and ANN led to a notable enhancement, raising the accuracy to 96.75%. These findings underline the effectiveness of incorporating diverse methodologies to address the inherent challenges in fault location for complex transmission configurations. This provides valuable insights for enhancing power grid reliability and maintenance despite the constraints posed by data availability.

In reference [9], the authors proposed a novel intelligent framework using a data logger-equipped design for fault classification and location in a smart distribution system. Their

approach incorporates over-current relays and Multi-Resolution Analysis (MRA) wavelet transform. However, the paper lacks clarification regarding selecting the faulted section within the system. Additionally, it is essential to note that their study has not considered the impact of joints between the cables. In [27], an amalgamation of pattern recognition methods and Fast Discrete S-Transform (FDST) was utilized in power transmission lines to detect the faults with improved accuracy and was also able to differentiate the interior faults from the external faults. For fault detection, the FDST technique uses current, voltage, and phase angles from both ends of the transmission line. However, the FDST technique in [27] is intricate and challenging in real-time applications. In [25], DWT, extract features from faulty voltage and current signals, and employ ANN in fault locations in an overhead transmission line. The most noteworthy drawbacks are its massive training data and lengthy training procedure, which add to the computational load. Additionally, owing to the inter-harmonics and decaying DC components, DWT is also impacted, which causes erroneous results.

A combination of impedance, DWT and SVM is used in [28] for fault classification in a 110km, jointed overhead-underground transmission line. Voltage and current signals from one side of the line were used for classification of only four types of faults. Authors in [29] applied DWT to classify faults in a transmission line. In their method, current signals from the receiving and sending end of the transmission line were used, to classify four types of faults. A limitation of this method is that, analyzing the signals from both ends of a transmission line brings about signal distortion that may affect the expected results. A single-ended travelling wave-based fault location method for power transmission systems where overhead lines are combined with underground cables is proposed in [29]. DWT is used to extract transient information of recorded voltages, and SVM is used to determine the fault section. The normalized wavelet energies of post-fault voltages are used as the input to the classifier. A classification accuracy of 82.22% was achieved for ten types of faults.

This paper explores different techniques for improving the accuracy of fault classification and location in power distribution systems. A hybridization of methodologies based on impedance, discrete wavelet transforms, artificial neural networks, and ANFIS was employed. These techniques were combined to develop two models for classifying and locating short circuit faults in a continuous jointed overhead and underground distribution line. The DWT technique was selected for signal processing for fault classification. The DWT (db4) mother wavelet was applied to the current signal from the sending end of the jointed distribution line. The resulting coefficients were combined with an MLP neural network for fault classification. Although SVM cascaded with DWT has shown some improvement in fault classification for long-distance transmission lines, it has some limitations in the number of faults classified, and, a threshold for fault value is required. Thus, an integration of MPL-DWT is adopted in this study, which does not require fault value thresholding in classification. An impedance-adaptive Neuro-Fuzzy System-based technique was applied for fault location.

The proposed technique's capability of classifying and locating 11 types of short circuit-related faults is also a significant contribution to the field of study. Additionally, the design focuses on jointed overhead and underground distribution lines, which, has received limited attention in previous researches. This emphasis makes the design highly relevant for practical applications in the power system distribution sector. Using conventional and soft computing techniques ensures the robustness and high accuracy of the system, providing an inclusive solution that overcomes the limitations of individual technique's designs. This research aims to leverage the strengths of both approaches in fault classification and location in a continuous combined overhead line and distribution cable.

METHOD

This section discusses an alternative approach to fault classification and location in a hybrid distribution topology. The hybrid distribution topology comprises two key elements: coordination of the fault categorization model and the fault location model. A DWT-MLP ANN model is proposed for fault classification, whereas an impedance-based ANFIS model is established for fault location.

Distribution Line Model

A distribution line model was established to classify faults and to evaluate the performance of algorithms designed for fault classification and location. A simplified single-line diagram of a 20 km, 11 kV jointed overhead and an underground power line is illustrated in Figure 1. The combined distribution line comprises a 15 km overhead line with a diameter of 150 mm² and a 5 km underground cable diameter of 300 mm².

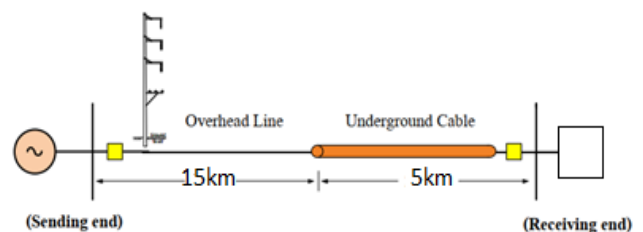


Figure 1. Simplified single line diagram

For further processing and evaluation, a simplified distribution line model was developed. This model was then expanded into a distributed parameter model to represent the overhead line and the underground cable system, as shown in Figure 2. In this model, a three-phase power source with a magnitude of 66 kV is connected to a 66/11 kV step-down transformer, which produces 11 kV for distribution.

Voltage and current measurements of the distribution system were taken from the bus bar at the sending end; these signals were utilized to verify how the system is affected by faults. The distribution line is sectionalized to enable fault introduction at different distances. The section blocks A, B, C, D, and E are fault blocks used to introduce fault into the model. They have been placed in sections to map the whole distribution line length. The overhead line (OHL) and underground cable (UGC) distributed parameters, shown in Table 1, were used to model the distribution line.

Table 1. Distribution system parameters

Components	Parameters
Three Phase Source	Resistance = 0.45Ω
	Inductance = 63.73 H
	Phase Voltage = 66 kV
66/11 kV Transformer	Nominal Power = 23 MVA
	Frequency = 50 Hz
Overhead Distribution Line	Resistance = $0.2228 \Omega/\text{km}$
	Inductance = $84.67 \mu\text{H}/\text{km}$
	Capacitance = $0.27724 \text{ nF}/\text{km}$
Underground Distribution Line	Resistance = $0.0796 \Omega/\text{km}$
	Inductance = $0.2833 \text{ mH}/\text{km}$
	Capacitance = $0.52 \mu\text{F}/\text{km}$
11/0.433 kV Transformer	Nominal Power = 630 kVA
	Frequency = 50 Hz
Load	Active Power = $262,721.79 \text{ W}$
	Reactive Power = 162.8 MVar

The established fault classification and location models involve the three-phase voltages and currents at the sending end of the hybrid distribution line. The model was designed in the MATLAB/Simulink platform, and data from simulations was processed for further use in either ANN or ANFIS, depending on the sub-model being executed.

Fault Classification

An assumption that a fault has already occurred is initially made to initiate fault classification. Single-phase, double-phase, and three-phase faults can occur on distribution lines; thus, these faults were created for analysis. Figure 3 depicts the developed model used to generate the fault signals for classifying and identifying faults. V_{abc} and I_{abc} are voltage and current signals from the sending end. The signals were passed through low pass filters (LPF), with a 50 Hz fundamental frequency for filtering out harmonics caused by the system's load and source inductance. Current signals were selected for analysis as they were the most affected system parameters when a fault occurs compared to the voltage signal.

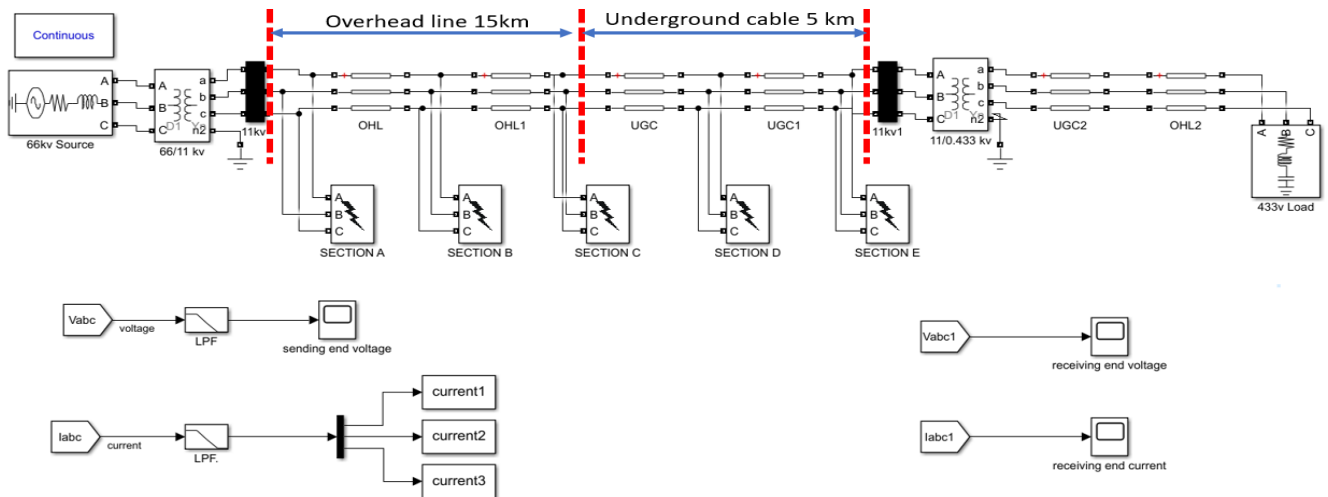


Figure 2. Combined overhead-underground distribution line model

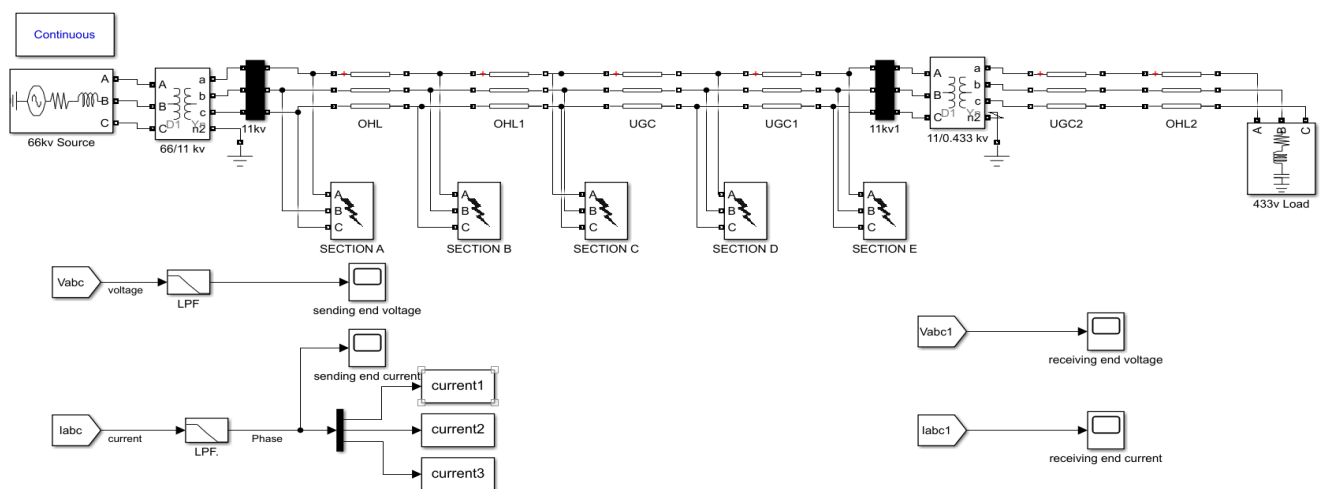


Figure 3. Combined overhead and underground distribution line model for fault classification

To perform the DWT-MLP ANN-based algorithm, the following steps were executed for the designed fault classification technique:

- i. A distribution system model was created using Simulink, and three-phase currents were measured at the sending end.
- ii. Utilizing DWT, 3rd level, and db4, phase current coefficients were derived from the three-phase current signals.
- iii. The detailed coefficients for each phase, as well as their maximum value, were determined and assumed as follows:
 S_a = Maximum detailed coefficient of phase A
 S_b = Maximum detailed coefficient of phase B
 S_c = Maximum detailed coefficient of phase C
- iv. Preprocessing the data: The phase coefficients and the type of fault data were used for the Neural Network development.
- v. Divided the data into train and test sets.
- vi. The types of faults: phase-ground, phase-phase, phase-phase-ground, three phases, and three phases-ground were labelled as shown in Table 2.
- vii. MLP network architecture was set by choosing the optimum: Hidden layers, activation function, the solver, learning rate, and maximum iteration.
- viii. Trained and tested the developed classification model.
- ix. A confusion matrix and percentage error after training and testing were obtained.

Table 2. Labels on type of faults

Type of Fault	Label
Phase A to Ground	1
Phase B to Ground	2
Phase C to Ground	3
Phase A and B	4
Phase A and C	5
Phase B and C	6
Phase AB to Ground	7
Phase AC to Ground	8
Phase BC to Ground	9
Phase A, B, and C	10
Phase ABC to Ground	11

A MATLAB code was developed to decompose current signals and determine the highest coefficient in each phase. At different

distances, phase current coefficients were collected for training and testing; a 3200 data set were used. The data was randomly split into two, with 20% of the data being applied to the classifier's predictions testing and 80% used for training. A model with 20 hidden layers was used and to activate the hidden layers an identity function activator was adopted. Optimization of the weights was achieved through a Limited-memory Broyden–Fletcher–Goldfarb–Shanno Algorithm (L-BFGS) solver with 300 maximum iterations since it has the capacity to converge faster and performs better as compared to Adams solver. To schedule for weight updates, a constant learning rate was utilized as it can be applied to complex non-linear problems and can also accommodate large input data at relatively faster performance. The flowchart for the established algorithm is highlighted in Figure 4 whilst Table 3 shows the MLP architecture.

A model with 20 hidden layers was used, and an identity function activator was adopted to activate the hidden layers. The weights were optimized through a Limited-memory Broyden–Fletcher–Goldfarb–Shanno Algorithm (L-BFGS) solver with 300 maximum iterations since it can converge faster and perform better than the Adams solver. A constant learning rate was utilized to schedule weight updates as it can be applied to complex non-linear problems and accommodate extensive input data at relatively faster performance. The flowchart for the established algorithm is highlighted in Figure 4, while Table 4 shows the MLP architecture, where N is the number of neurons in each hidden layer.

The accuracy of an MLP neural network model is influenced by three main factors: the number of hidden layers, the activation function used in the hidden layers, and the solver algorithm employed to optimize the model parameters [30]. This study examined several possible combinations of these factors and their corresponding accuracy percentages to identify the best MLP classifier model for fault classification. The performance metrics for each combination of factors and varying numbers of neurons (N) in each hidden layer are presented in Table 4. By analyzing the outcomes in Table 4, the optimal configuration of the MLP model was determined to be N = 20, Identity activation function, and Lbfs solver, which achieved an accuracy of 96.67%. This outcome indicates that the proposed hybrid model, which employs the optimized MLP classifier, can accurately classify faults in distribution networks.

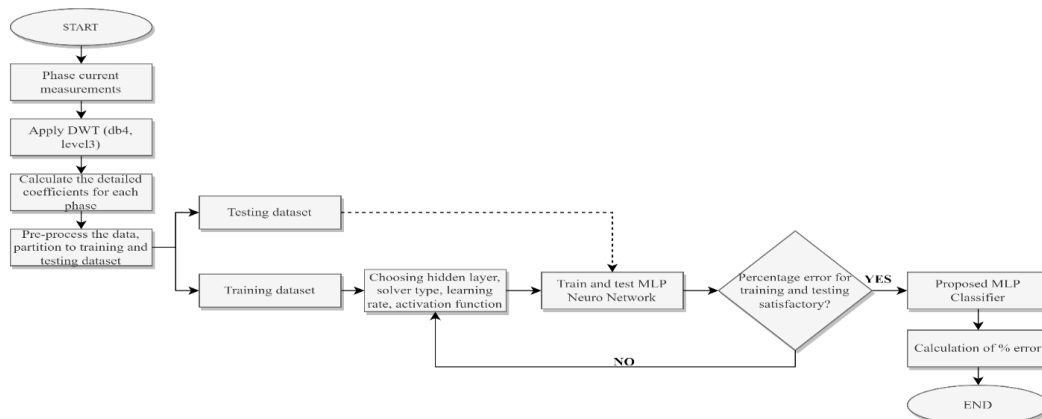


Figure 4. Fault classification flowchart.

Table 3. MLP-ANN training and testing sample data from DWT.

S. No	Sa	Sb	Sc	Fault Type
1	0.0374	0.0387	0.0356	No-Fault
2	0.1128	0.0364	0.0388	AG (Phase-Ground)
3	0.0406	0.1166	0.0360	BG (Phase-Ground)
4	0.0374	0.0390	0.1087	CG (Phase-Ground)
5	0.0777	0.0444	0.0375	AB (Phase-Phase)
6	0.0641	0.0433	0.0871	AC (Phase-Phase)
7	0.0413	0.0856	0.0649	BC (Phase-Phase)
8	0.1299	0.1453	0.0407	ABG (Phase-Phase-Ground)
9	0.1249	0.0512	0.1368	ACG (Phase-Phase-Ground)
10	0.0322	0.1236	0.1242	BCG (Phase-Phase-Ground)
11	0.0849	0.0713	0.0846	ABC (Three Phase)
12	0.1341	0.0946	0.12473	ABCG (Three Phase-Ground)

Table 4. Multi-layer perceptron architecture

Number of Neurons	Activation Function	Solver	Accuracy (%)
20	Logistic	L-BFGS	96.36
10, 20, 30	Logistic	SGD	9.09
50, 30, 10	Logistic	Adams	9.10
20	Tanh	L-BFGS	96.33
10, 20, 30	Tanh	SGD	39.70
50, 30, 10	Tanh	Adams	96.51
20	Identity	L-BFGS	96.67
10, 20, 30	Identity	SGD	44.09
50, 30, 10	Identity	Adams	96.00
20	Relu	L-BFGS	96.18
10, 20, 30	Relu	SGD	15.00
50, 30, 10	Relu	Adams	95.00

ANFIS-based Fault Location Model

This study uses the one-ended impedance fault location approach. This technique does not encounter any reflection of signals compared to other fault location methods, such as double-ended impedance. Phase-to-ground voltage measurements were used to calculate the impedance at the sending end. When compared to phase-to-phase voltage and current measurements, the phase-to-ground voltage and current measurements showed a significant difference in the current and voltage measurements when a fault was introduced. The phase impedance measurements were employed as the input to the ANFIS for training and testing the

model for fault location. A dataset of 1000 simulated fault data from impedance calculations was used, with 80% of the dataset being used to train the ANFIS, and 20% of the dataset was used to test the system's performance. The following steps were carried out in the developed fault location technique to execute the Impedance-ANFIS-based algorithm:

- i. Phase-to-ground currents and voltages were measured at the sending end.
- ii. Impedance was calculated.
- iii. Preprocessing the data: the phase impedance and the distance for the ANFIS development.
- iv. Divided the data into train and test sets.
- v. ANFIS network architecture was set by choosing the optimum: membership function, the number of epochs, type of membership function, and output membership function type.
- vi. Trained and tested the developed location model.
- vii. Percentage error after training and testing calculation.

Figure 5 illustrates the associated flowchart for developing the fault classification model. Figure 6 shows the model developed for fault location, considering the phase-to-ground voltage and current for impedance calculations V_{abc} and I_{abc} are the voltage and current measurements utilized for impedance calculation per phase. The output was connected to the ANFIS model developed for fault location, and the predicted distance was then displayed.

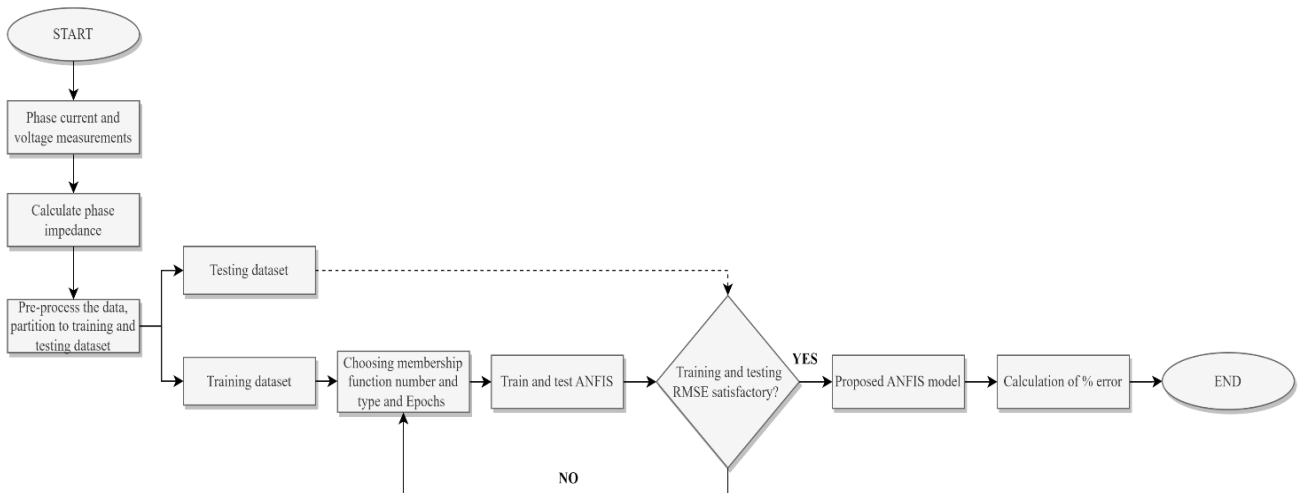


Figure 5. Fault location flowchart.

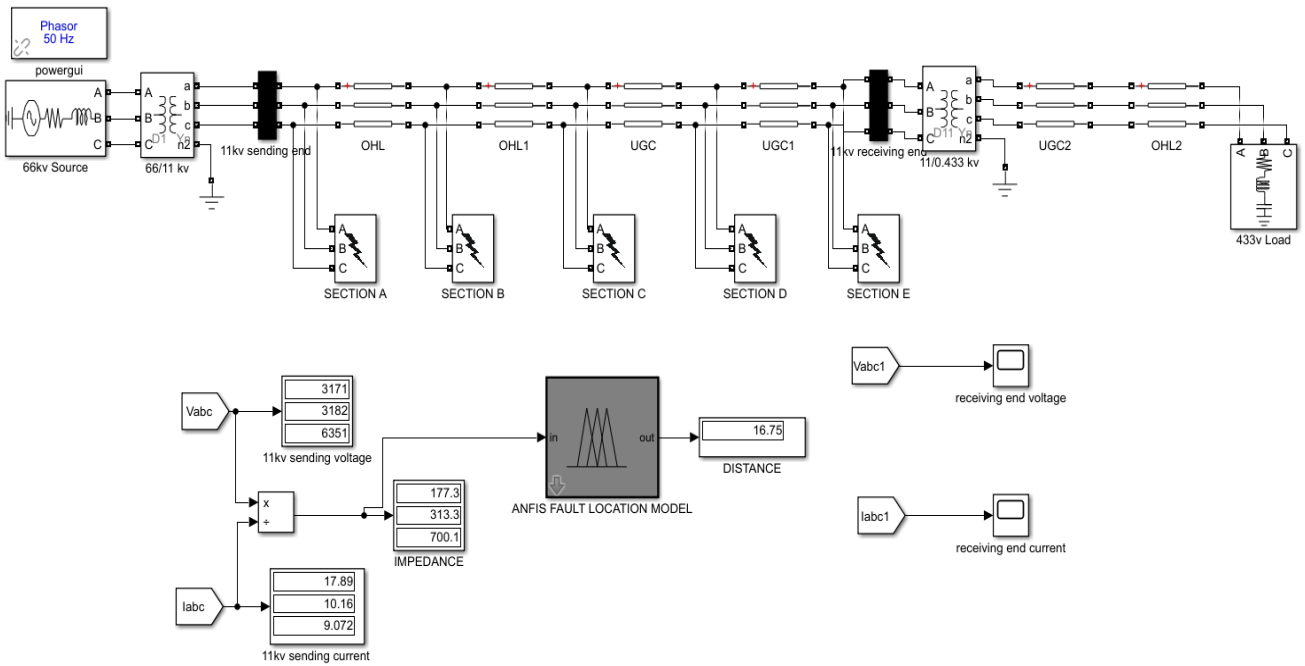


Figure 6. Combined Overhead and Underground distribution line model for fault location

Table 5. Sample training data from impedance calculations.

Type of fault	Impedance Phase A (Ω)	Impedance Phase B (Ω)	Impedance Phase C (Ω)
AG (Phase-Ground)	3.355	700.7	699.9
BG (Phase-Ground)	699.9	3.355	700.7
CG (Phase-Ground)	700.7	699.9	3.355
AB (Phase-Phase)	176.4	310.3	700.1
AC (Phase-Phase)	310.3	700.1	176.4
BC (Phase-Phase)	700.1	176.4	310.3
ABG (Phase-Phase-Ground)	4.739	4.11	806.5
ACG (Phase-Phase-Ground)	4.11	806.5	4.739
BCG (Phase-Phase-Ground)	806.5	4.739	4.11
ABC (Three Phase)	1.736	1.736	1.736
ABCG (Three Phase-Ground)	1.736	1.736	1.736

For illustration, Table 5 displays a sample of the obtained impedance values at 5 km (overhead distribution line side). The highlighted values in bold are of the faulted phase. The affected phase is observed to have low-value impedance ranging between 1.5 Ω to 310 Ω since when a fault occurs, current peaks and the voltage falls, leading to low impedance. Also, the three-phase and three-phase ground faults have the same values in impedance because they are symmetrical faults, which means current and voltage during the fault will be symmetrically distributed, leading to the same impedance in each phase.

Figure 7 shows the generated ANFIS model structure for fault location, where the input variables are the impedance values of each phase, and the output is the predicted fault distance. ANFIS was preferred because it presents a better learning ability and adaptability. The membership function influences the efficacy and computational cost of the ANFIS-based model; the triangular membership function showed better results for this study. The training of the system is depicted in Figure 8. The goal was to create a model that, given the distribution line fault signals, can precisely estimate the fault location. Figure 9 illustrates the error for testing the system and showcasing any anomalies to

evaluate the training's efficacy, while the rules generated after training are shown in Figure 10.

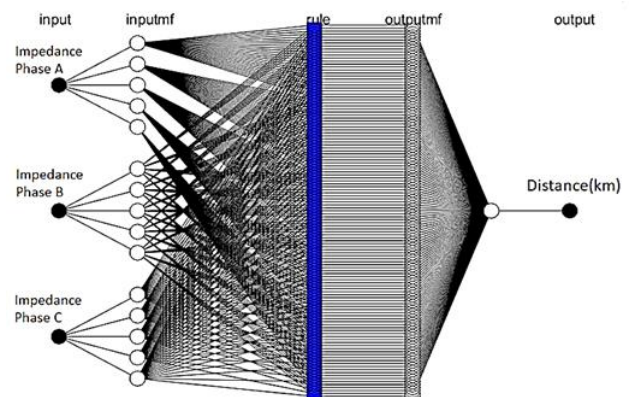


Figure 7. Generated ANFIS model structure.

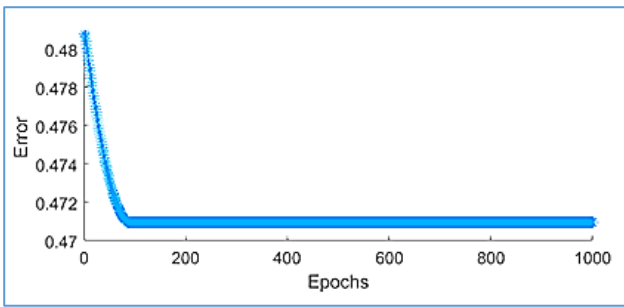


Figure 8. Training error of the dataset.

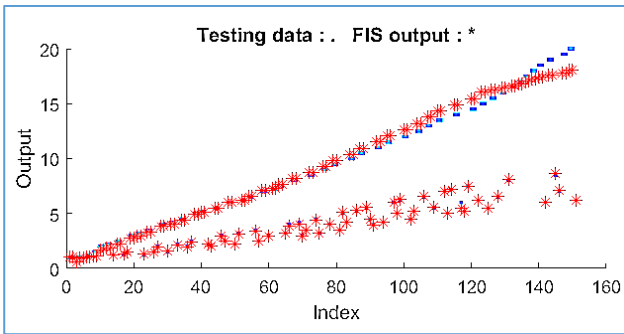


Figure 9. Testing error of the dataset.

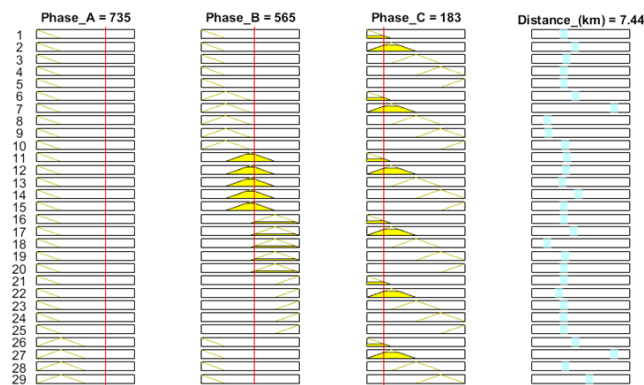


Figure 10. ANFIS Rule viewer.

RESULTS AND DISCUSSION

This section assesses the performance of the suggested methodologies under various fault scenarios and presents the findings.

Fault Identification and Classification

The results categorize the fault type based on the signals acquired from the jointed overhead-underground distribution line's sending end. After fault introduction, each phase current is affected differently depending on the type of fault. Figure 11 shows the confusion matrix that indicates the number of actual classes and projected class predictions made by the fault classification

algorithm. The matrix evaluates the algorithm's performance, showing the accuracy of the algorithm in predicting the correct class for each sample in the test set. The matrix rows signify the samples' actual fault classes, and the columns characterize the predicted fault classes. The entries in the matrix indicate the percentage of samples that were predicted to belong to each combination of actual and predicted classes. A confusion matrix as a percentage is used to ease visualization and compare the performance of the classification algorithm across different classes. Table 6 shows how the MLP classifier classified each fault type with a mean accuracy of 96.7%. The results demonstrated that the established fault classification system has an improved accuracy level compared to observations in [31].

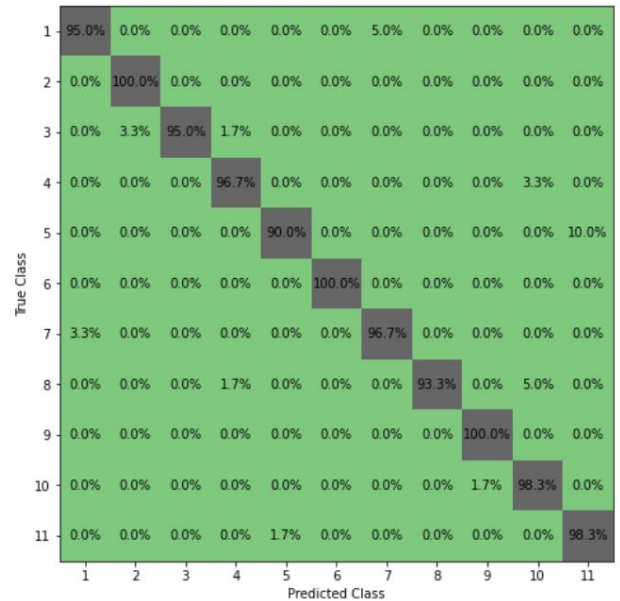


Figure 11. Fault classification algorithm confusion matrix.

Table 6. MLP Classifier Percentage Accuracy.

Type of Fault	Class Label	Accuracy (%)
AG (Phase-Ground)	1	95.0
BG (Phase-Ground)	2	100.0
CG (Phase-Ground)	3	95.0
AB (Phase-Phase)	4	96.7
AC (Phase-Phase)	5	90.0
BC (Phase-Phase)	6	100.0
ABG (Phase-Phase-Ground)	7	96.7
ACG (Phase-Phase-Ground)	8	93.3
BCG (Phase-Phase-Ground)	9	100.0
ABC (Three Phase)	10	98.3
ABCG (Three Phase-Ground)	11	98.3
Mean Accuracy		96.7

Table 7. Comparison of some fault classification techniques.

S. No	Method	Parameters	Type of System	Faults	Accuracy
1	Impedance, DWT, and SVM[28]	Voltage and current single-ended	110 km, jointed overhead-underground transmission line	4	99.01%
2	DWT[31]	current signal from the sending and receiving end of the line	40 km, 115 kV overhead-underground transmission line	4	82.22%
3	DWT-SVM [29]	Voltage signal, single-ended	194 km, 120 kV overhead-underground transmission line	10	99.10%
4	Traveling wave (DWT) [32]	Voltage signal, single-ended	322 km, 230 kV overhead-underground transmission line	3	98.30%
5	DWT-MLP Neural Network (proposed)	Current	20 km, 11 kV overhead-underground distribution line	11	96.70%

The fault classification system developed in this study achieved a higher accuracy than [31], attributed to the hybridization of discrete wavelet transforms and MLP artificial neural network techniques. Although results from references [28], [30], and [32] have high percentage classification accuracy compared to the proposed model, they classified fewer faults, and their application was towards jointed overhead-underground transmission lines. The proposed system classified 11 types of short circuit faults, and its accuracy is comparable to the previous studies, which is also a notable improvement over previous studies in [28] – [30], [32], as seen in Table 7. These improvements make the fault classification system a valuable addition to fault classification in jointed overhead-underground power distribution systems, potentially enhancing their accuracy and efficiency.

Fault Location

The fault location algorithm in this study used impedance data calculated for each phase. This data was used in training and testing the ANFIS system for fault location. A graphical user interface (GUI) was established to facilitate the implementation of AFIS for fault location. A simulated data set of 1,000 samples was created to develop and fine-tune the fault location algorithm. In Tables 8 and 9, an illustration of how the system performs based on the effect of the type of fault for the same distance is assessed. The percentage error in fault location prediction is determined by pointing at different types of faults at randomly selected distances of 8 km in the overhead line and 16.5 km underground cable (from the sending end). Table 8 shows that the BCG (phase-phase-ground) fault had a maximum error of magnitude 2.75%. Results for fault location prediction in underground cable for all types of faults at 16.5 km are presented in Table 9. The maximum error recorded for this selected distance is 0.7078% for the three-phase faults.

Table 10 displays the results of the simulations performed at arbitrary fault locations chosen on the line to establish the accuracy of the developed ANFIS model. The percentage error of each predicted outcome was established and shown using Equation 1, in which negative values observed result from the predicted distance exceeding the actual distance.

Table 8. Location prediction based on Fault type in the overhead line section.

Type of Fault	Actual distance (km)	Predicted distance (km)	Difference (km)	Error (%)
AG	8	8.01	0.01	0.125
BG	8	8.17	0.17	2.125
CG	8	8.22	0.22	2.750
AB	8	8.13	0.13	1.625
AC	8	8.17	0.17	2.125
BC	8	8.18	0.18	2.250
ABG	8	8.13	0.13	1.625
ACG	8	8.13	0.13	1.625
BCG	8	8.22	0.22	2.750
ABC	8	8.07	0.07	0.875
ABCG	8	8.07	0.07	0.875
AVERAGE			0.136	1.704

Table 9. Location prediction based on Fault type in underground cable section.

Type of Fault	Actual Distance (Km)	Predicted Distance (Km)	Difference (Km)	Error (%)
AG	16.5	16.44	-0.06	-0.3636
BG	16.5	16.44	-0.06	-0.3636
CG	16.5	16.49	-0.01	-0.0606
AB	16.5	16.49	-0.01	-0.0606
AC	16.5	16.49	-0.01	-0.0606
BC	16.5	16.49	-0.01	-0.0606
ABG	16.5	16.49	-0.01	-0.0606
ACG	16.5	16.51	0.01	0.0606
BCG	16.5	16.52	0.02	0.1212
ABC	16.5	16.63	0.13	0.7878
ABCG	16.5	16.63	0.13	0.7878
AVERAGE			0.01181	0.0661

Table 10. Fault Location and Error Estimation

Section	Actual Distance (Km)	Predicted Distance (Km)	Difference (Km)	Error (%)
Overhead	1.20	1.29	0.09	7.500
	2.50	2.44	-0.06	-2.400
	3.20	3.18	-0.02	-0.625
	4.57	4.60	0.03	0.656
	5.30	5.20	-0.10	-1.880
	6.27	6.40	0.13	2.070
	7.02	7.00	-0.02	-0.285
	8.22	8.10	-0.12	-1.450
	9.09	9.10	0.01	0.001
	10.38	10.13	-0.25	-2.410
	11.05	11.00	-0.05	-0.452
	12.06	11.50	-0.56	-4.640
	13.00	13.30	0.30	2.300
	14.33	14.67	0.34	2.370
Average				0.054
Underground	15.47	15.21	-0.26	-1.680
	16.01	16.00	-0.01	-0.062
	17.58	17.50	-0.08	-0.455
	18.50	18.68	0.18	0.973
	19.50	19.80	0.30	1.538
Average				0.063
Overall Average percentage error				0.056

Table 11. Comparison of some on-fault location techniques

No	Technique	Parameters	Type of System	Accuracy
1	Modal transformation method [3].	Voltage and current from both the sending and receiving end.	Single line, 400kV, 110km overhead-underground transmission line	95.00%
2	Wavelet transform and ANN [3].	Voltage and current from both the sending and receiving end.	Single line, 400kV, 110km overhead-underground transmission line	96.75%
3	Travelling wave with data loggers [9]	Voltage	13-node network, 20kV overhead-underground distribution line	98.50%
4	Impedance, DWT, and SVM [28]	Voltage and current single-ended	110km, overhead-underground transmission line	99.88%
5	Impedance-ANFIS (Proposed)	Voltage and Current signal	20km, 11kV overhead-underground distribution line	99.17%

The error histogram in Figure 12 graphically represents the distribution of errors in the fault location model predictions. It visualizes the model's accuracy by showing the frequency of errors at different levels of magnitude. The errors are first computed by taking the variance between the model's predicted values and the target variable's actual values for each observation in the dataset. These errors are then binned into a set of bins, and the total errors in each bin are counted. The total counts are plotted on the y-axis, and the bins are plotted on the x-axis. A mean error of 0.0083 was obtained using Equation 2 from the error histogram.

$$Error(\%) = \frac{(\text{Predicted distance} - \text{Actual distance})}{\text{Actual distance}} \quad (1)$$

$$Mean Error = \frac{1}{n} \sum_{i=1}^n |\text{Predicted distance} - \text{Actual distance}| \quad (2)$$

where n is the number of observations in the dataset.

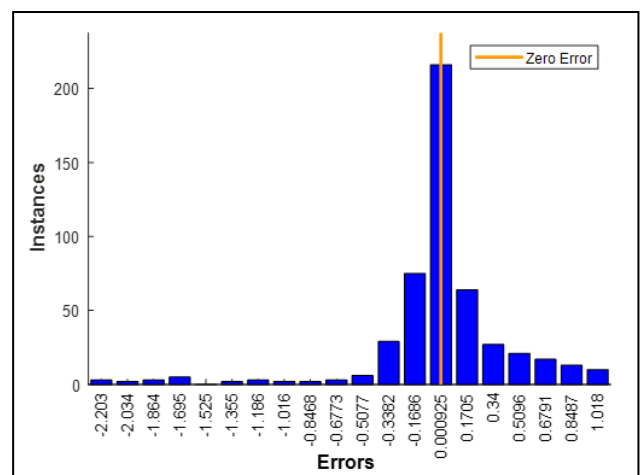


Figure 12. Predicted distance error histogram.

A mean error of 0.0083 represents a percentage accuracy of the fault location system of 99.17%, showing that all eleven (11) short circuit faults were accurately located along the distribution line. The algorithm developed in this study performed better than those presented in [3] and [9]. However, authors in [28] obtained a higher percentage accuracy but their study was limited to only four (4) types of faults classified and located. The proposed technique in this paper represents an improvement over the method established in [3] by incorporating ANFIS, which significantly enhanced fault location accuracy, as evidenced by the comparison with previous work presented in Table 11. It is important to note that the comparison was only performed on techniques used in fault location for combined overhead-underground transmission lines and jointed overhead-underground distribution lines. The proposed method significantly benefits distribution systems as it can classify and locate the 11 short circuit-related faults, enabling faster restoration times and reducing downtime.

CONCLUSIONS

This paper presents a hybrid technique for fault classification and location in a jointed overhead-underground distribution line. The designed model consists of two phases: fault type classification and fault location. The faults in the power distribution line were classified using a combination of DWT and MLP neuro-network models. While, the impedance-ANFIS-based approach was applied for fault location. The developed hybrid model managed to classify and locate 11 short circuit faults with higher accuracy. Fault classification was performed using phase coefficients from current signal analysis using DWT db4 at level three to train the MLP neuro network model. After training and testing, the classification model attained an average percentage error of 3.3%. Fault location was carried out using phase-to-ground impedance measurements at the sending end to train and test the ANFIS model, and the system percentage error was 0.83%. According to the simulation results, the developed model effectively classifies the fault type and can pinpoint the fault location with minimum error. Comparing key performance indicators of traditional and soft computing methods, the results of this study suggest that hybridizing with intelligent technology can significantly reduce system error margins.

Utility companies can deploy this hybrid technique to enhance outage management systems, deliver faster response times, and reduce downtime during a power outage. Maintenance planning becomes more efficient with accurate data, allowing utility companies to schedule repairs and proactively minimize customer disruption. Ultimately, this research enhances engineering capabilities to classify and locate faults while providing solutions that directly benefit power distribution operations and their customers.

ACKNOWLEDGMENT

The authors thank the Dedan Kimathi University of Technology for this research's financial and material support.

REFERENCES

- [1] M. A. Gabr, D. K. Ibrahim, E. S. Ahmed, and M. I. Gilany, "A new impedance-based fault location scheme for overhead unbalanced radial distribution networks," *Electric Power Systems Research*, vol. 142, pp. 154–162, Jan. 2017.
- [2] K. Wang, Z. Li, and B. Zhang, "A novel method of power cable fault monitoring," in *2016 IEEE PES Asia-Pacific Power and Energy Engineering Conference (APPEEC)*, 2016, pp. 738–742. doi: 10.1109/APPEEC.2016.7779653.
- [3] P. Ray, S. R. Arya, and D. P. Mishra, "Intelligence Scheme for Fault Location in a Combined Overhead Transmission Line & Underground Cable," *International Journal of Emerging Electric Power Systems*, vol. 19, no. 5, 2018, doi: 10.1515/ijeeps-2017-0277.
- [4] S. Shilpa G, H. Mokhlis, and H. Illias, "Fault location and detection techniques in power distribution systems with distributed generation: A review," *Renewable and Sustainable Energy Reviews*, vol. 74, pp. 949–958, Jul. 2017, doi: 10.1016/j.rser.2017.03.021.
- [5] A. Prasad, J. Belwin Edward, and K. Ravi, "A review on fault classification methodologies in power transmission systems: Part—I," *Journal of Electrical Systems and Information Technology*, vol. 5, no. 1, pp. 48–60, 2018, doi: 10.1016/j.jesit.2017.01.004.
- [6] K. Chen, C. Huang, and J. He, "Fault detection, classification and location for transmission lines and distribution systems: a review on the methods," *High Voltage*, vol. 1, no. 1, pp. 25–33, 2016, doi: 10.1049/hve.2016.0005.
- [7] M. Daisy and R. Dashti, "Single phase fault location in electrical distribution feeder using hybrid method," *Energy*, vol. 103, pp. 356–368, 2016, doi: https://doi.org/10.1016/j.energy.2016.02.097.
- [8] R. Dashti and J. Sadeh, "Accuracy improvement of impedance-based fault location method for power distribution network using distributed-parameter line model," *International Transactions on Electrical Energy Systems*, vol. 24, no. 3, pp. 318–334, Mar. 2014, doi: https://doi.org/10.1002/etep.1690.
- [9] S. Khavari, R. Dashti, H. R. Shaker, and A. Santos, "High Impedance Fault Detection and Location in Combined Overhead Line and Underground Cable Distribution Networks Equipped with Data Loggers," *Energies (Basel)*, vol. 13, no. 9, p. 2331, 2020, doi: 10.3390/en13092331.
- [10] A. H. A. Bakar, M. S. Ali, C. Tan, H. Mokhlis, H. Arof, and H. A. Illias, "High impedance fault location in 11kV underground distribution systems using wavelet transforms," *International Journal of Electrical Power & Energy Systems*, vol. 55, pp. 723–730, 2014, doi: https://doi.org/10.1016/j.ijepes.2013.10.003.
- [11] M. Goudarzi, B. Vahidi, R. A. Naghizadeh, and S. H. Hosseinian, "Improved fault location algorithm for radial distribution systems with discrete and continuous wavelet analysis," *International Journal of Electrical Power & Energy Systems*, vol. 67, pp. 423–430, 2015, doi: https://doi.org/10.1016/j.ijepes.2014.12.014.

- [12] H. Jia, "An Improved Traveling-Wave-Based Fault Location Method with Compensating the Dispersion Effect of Traveling Wave in Wavelet Domain," *Math Probl Eng*, vol. 2017, pp. 1–11, 2017, doi: 10.1155/2017/1019591.
- [13] J. Han and P. A. Crossley, "Traveling wave fault locator for mixed, overhead, and underground teed transmission feeders," *IEEJ Transactions on Electrical and Electronic Engineering*, vol. 10, no. 4, pp. 383–389, 2015, doi: 10.1002/tee.22097.
- [14] Y. Aslan and Y. E. Yağan, "Artificial neural-network-based fault location for power distribution lines using the frequency spectra of fault data," *Electrical Engineering*, vol. 99, no. 1, pp. 301–311, 2017, doi: 10.1007/s00202-016-0428-8.
- [15] S. S. Gururajapathy, H. Mokhlis, H. A. Bin Illias, and L. J. Awalin, "Support vector classification and regression for fault location in distribution system using voltage sag profile," *IEEJ Transactions on Electrical and Electronic Engineering*, vol. 12, no. 4, pp. 519–526, Jul. 2017, doi: <https://doi.org/10.1002/tee.22407>.
- [16] A. Hossam-Eldin, A. Lotfy, M. Elgamal, and M. Ebeed, "Combined traveling wave and fuzzy logic based fault location in multi-terminal HVDC systems," in *2016 IEEE 16th International Conference on Environment and Electrical Engineering (EEEIC)*, 2016, pp. 1–6. doi: 10.1109/EEEIC.2016.7555591.
- [17] S. Adhikari, N. Sinha, and T. Dorendrajit, "Fuzzy logic based on-line fault detection and classification in transmission line," *Springerplus*, vol. 5, no. 1, p. 1002, 2016, doi: 10.1186/s40064-016-2669-4.
- [18] P. P. Bedekar, S. R. Bhide, and V. S. Kale, "Fault section estimation in power system using Hebb's rule and continuous genetic algorithm," *International Journal of Electrical Power & Energy Systems*, vol. 33, no. 3, pp. 457–465, 2011, doi: <https://doi.org/10.1016/j.ijepes.2010.10.008>.
- [19] J. Qiyan and J. Rong, *Fault Location for Distribution Network Based on Genetic Algorithm and Stage Treatment*. 2012. doi: 10.1109/SCET.2012.6342090.
- [20] E. E. Ngu and K. Ramar, "A combined impedance and traveling wave based fault location method for multi-terminal transmission lines," *International Journal of Electrical Power & Energy Systems*, vol. 33, no. 10, pp. 1767–1775, 2011, doi: 10.1016/j.ijepes.2011.08.020.
- [21] O. A. S. Youssef, "Combined fuzzy-logic wavelet-based fault classification technique for power system relaying," *IEEE Transactions on Power Delivery*, vol. 19, no. 2, pp. 582–589, 2004, doi: 10.1109/TPWRD.2004.826386.
- [22] J. Klomjit and A. Ngaopitakkul, "Selection of proper input pattern in fuzzy logic algorithm for classifying the fault type in underground distribution system," in *2016 IEEE Region 10 Conference (TENCON)*, 2016, pp. 2650–2655. doi: 10.1109/TENCON.2016.7848519.
- [23] J. Sadeh and H. Afradi, "A new and accurate fault location algorithm for combined transmission lines using Adaptive Network-Based Fuzzy Inference System," *Electric Power Systems Research*, vol. 79, no. 11, pp. 1538–1545, 2009, doi: 10.1016/j.epsr.2009.05.007.
- [24] J. Moshtagh and R. K. Aggarwal, "A new approach to fault location in a single core underground cable system using combined fuzzy logic and wavelet analysis," in *2004 Eighth IEE International Conference on Developments in Power System Protection*, 2004, pp. 228–231 Vol.1. doi: 10.1049/cp:20040105.
- [25] A. Yadav and A. Swetapadma, "A single ended directional fault section identifier and fault locator for double circuit transmission lines using combined wavelet and ANN approach," *International Journal of Electrical Power & Energy Systems*, vol. 69, pp. 27–33, 2015, doi: <https://doi.org/10.1016/j.ijepes.2014.12.079>.
- [26] C. K. Jung, K. H. Kim, J. B. Lee, and B. Klöckl, "Wavelet and neuro-fuzzy based fault location for combined transmission systems," *International Journal of Electrical Power & Energy Systems*, vol. 29, no. 6, pp. 445–454, 2007, doi: 10.1016/j.ijepes.2006.11.003.
- [27] K. R. Krishnanand, P. K. Dash, and M. H. Naeem, "Detection, classification, and location of faults in power transmission lines," *International Journal of Electrical Power & Energy Systems*, vol. 67, pp. 76–86, 2015, doi: <https://doi.org/10.1016/j.ijepes.2014.11.012>.
- [28] J. Tavalaei, M. H. Habibuddin, A. Khairuddin, and A. A. Mohd Zin, "Fault Location and Classification of Combined Transmission System: Economial and Accurate Statistic Programming Framework," *J Electr Eng Technol*. 2017, pp. 2106–2116, 2017, doi: <http://doi.org/10.5370/JEET.2017.12.6.2106>.
- [29] H. Livani and C.Y. Evrenosoglu, "A Hybrid Fault Location Method for Overhead Lines Combined with Underground Cables Using DWT and SVM," *IEEE*, pp. 1–6, 2012.
- [30] M. Dashtdar, M. Esmaeilbeig, M. Najafi, and M. E. N. Bushehri, "Fault Location in the Transmission Network Using Artificial Neural Network," *Automatic Control and Computer Sciences*, vol. 54, no. 1, pp. 39–51, 2020, doi: 10.3103/s0146411620010022.
- [31] J. Klomjit and A. Ngaopitakkul, "Fault Classification on the Hybrid Transmission Line System Between Overhead Line and Underground Cable," in *IFSA-SCIS 2017*, Otsu, Shiga, Japan: IEEE, Jun. 2017.
- [32] H. Livani and C.Y. Evrenosogl, "A Traveling Wave Based Single-Ended Fault Location Algorithm using DWT for Overhead Lines Combined with Underground Cables," *IEEE*, 2010.